**Atmospheric
Chemistry
and Physics
Discussions**

Secondary organic material formed by methylglyoxal in aqueous aerosol mimics – Part 2: Product identification using Aerosol-CIMS

N. Sareen, E. L. Shapiro, A. N. Schwier, and V. F. McNeill

Department of Chemical Engineering, Columbia University, New York, NY, USA

Correspondence to: V. F. McNeill (vfm2103@columbia.edu)

Abstract

We used chemical ionization mass spectrometry with a volatilization flow tube inlet (Aerosol-CIMS) to characterize secondary organic material formed by methylglyoxal with ammonium sulfate in aqueous aerosol mimics. Bulk reaction mixtures were di-
5 luted and atomized to form submicron aerosol particles. Organics were detected using Aerosol-CIMS in positive and negative ion mode using I^- and $H_3O^+ \cdot (H_2O)_n$ as reagent ions. The results are consistent with aldol condensation products, carbon-nitrogen species, sulfur-containing compounds, and oligomeric species up to 759 amu. These results support previous observations by us and others that ammonium sulfate plays a
10 critical role in the SOA formation chemistry of dicarbonyl compounds.

1   Introduction

There is growing evidence that carbonyl-containing compounds participate in secondary organic aerosol (SOA) formation via heterogeneous uptake to aqueous aerosol particles (Jang et al., 2005; Liggio et al., 2005a, b; Volkamer et al., 2006, 2007, 2009;
15 Loeffler et al., 2006; Zhao et al., 2006; Gao et al., 2006; Nozière et al., 2009; Fu et al., 2009; Shapiro et al., 2009; Galloway et al., 2009; De Haan et al., 2009a, b). Secondary organic products can affect the optical properties (Saathoff et al., 2003; Casale et al., 2007; Nozière and Esteve, 2007; Nozière et al., 2007, 2009; Shapiro et al., 2009; De Haan et al., 2009a), CCN activity (Cruz and Pandis, 1997; Hartz et al., 2005; King et al.,
20 2007; Duplissy et al., 2008; Michaud et al., 2009), and heterogeneous chemistry (Folkers et al., 2003; Anttila et al., 2006) of the seed aerosol. A variety of SOA products have been proposed for these processes, including organosulfates, carbon-nitrogen species, and aldol condensation products.

Methylglyoxal ($C_3H_4O_2$), a volatile α-dicarbonyl, is an oxidation product of many
25 volatile organic compounds (Tuazon et al., 1986; Grosjean et al., 1993; Smith et al., 1999). Methylglyoxal may participate in heterogeneous SOA formation via the for-

mation of acetal and hemiacetal oligomers (Nemet et al., 2004; Kalberer et al., 2004; Paulsen et al., 2005; Loeffler et al., 2006; Zhao et al., 2006; Krizner et al., 2009) or aldol condensation (Barsanti and Pankow, 2005; Krizner et al., 2009). We report in a companion paper that methylglyoxal forms light-absorbing and suface-active products in aqueous solution with ammonium salts (Schwier et al., 2009). Our results suggest the formation of aldol condensation products and a mechanism involving participation of the ammonium ion. A proposed reaction scheme is shown in Fig. 1.

Chemical ionization mass spectrometry coupled with a volatilization flow tube inlet (Aerosol-CIMS) enables measurements of aerosol composition simultaneously with gas-phase composition, with the high sensitivity, selectivity, and fast time response of CIMS (Hearn and Smith, 2004a; McNeill et al., 2007, 2008). Aerosol-CIMS allows speciated measurements of aerosol organics which are selective based on the choice of parent ion. Chemical ionization is a relatively soft ionization technique that results in low fragmentation of organics, thus simplifying their identification and quantification. Aerosol-CIMS has been used for laboratory studies of the oxidative aging of organic aerosols (Hearn and Smith, 2004b, 2005, 2006a, 2007; Hearn et al., 2005, 2007; McNeill et al., 2007, 2008) and to characterize aerosols of complex chemical composition (Hearn and Smith, 2006b).

We have characterized the reaction products of methylglyoxal in aqueous solution with $(NH_4)_2SO_4$ and NaCl by atomization of diluted reaction mixtures followed by Aerosol-CIMS detection in both positive and negative ion mode. The two reagent ions used, I^- and $H_3O^+ \cdot (H_2O)_n$, are complementary in their versatility ($H_3O^+ \cdot (H_2O)_n$) and selectivity (I^-). We find evidence of aldol condensation products, sulfur-containing compounds, carbon-nitrogen species, and high-molecular-weight oligomeric species. These results add to the growing body of evidence that dicarbonyl compounds form SOA material in the aqueous phase, and that ammonium sulfate plays an active role in the SOA formation mechanisms (Liggio et al., 2005a, b; Nozière et al., 2009; Shapiro et al., 2009; Galloway et al., 2009; Schwier et al., 2009).

15569

2 Methods

2.1 Aerosol-CIMS

Experiments were conducted using a custom-built Aerosol-CIMS apparatus. Analyte molecules were detected as the products of their interactions with I^- or $H_3O^+ \cdot (H_2O)_n$ using a quadrupole mass spectrometer with high mass (≤ 1000 amu) capabilities (Extrel CMS). A schematic of the experimental system is shown in Fig. 2.

Mixtures initially containing 1.62 M methylglyoxal and 3.1 M $(NH_4)_2SO_4$ or 5.1 M NaCl with pH=2 were prepared using Millipore water as described in Schwier et al. (2009). After the desired reaction time had passed, the mixtures were diluted with Millipore water until the salt concentration was 0.2 M. Reaction time was generally >24 h, which was sufficient time for significant light absorption and surface tension depression to develop in the methylglyoxal/$(NH_4)_2SO_4$ solutions as reported in the companion paper (Schwier et al., 2009). Reaction kinetics at short times were investigated as follows: a small amount of reaction mixture initially containing 1.62 M methylglyoxal and 3.1 M $(NH_4)_2SO_4$ was diluted 2 min after mixing. Another sample of the same bulk reaction mixture was diluted 38 min after mixing. The mass spectra of these samples were measured using Aerosol-CIMS immediately after dilution.

Control experiments were performed in which a 0.2 M $(NH_4)_2SO_4$ solution at pH=2 was atomized and analyzed using Aerosol-CIMS. Additional control experiments to test the performance of Aerosol-CIMS in the high mass detection mode were performed using a solution of 0.2 M NaCl and 3.9 mM poly(ethylene glycol) (PEG) (Sigma Aldrich, 570–630 amu) in Millipore water.

The dilute solutions were aerosolized with N_2 using a constant output atomizer (TSI 3076), forming submicron particles. The aerosol stream was combined with a dry N_2 dilution flow, resulting in a relative humidity of 50–60% as measured with a hygrometer (Vaisala). The particle population was characterized using a scanning mobility particle sizer (SMPS) (Grimm Technologies, TSI). The aerosol had a lognormal size distribution with a typical geometric standard deviation of 1.8 and a mean volume-weighted
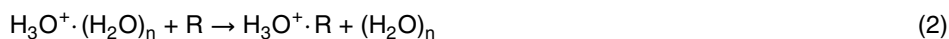
15570

particle radius of 119±1 nm. Typical number concentrations were $\sim 7 \times 10^4$ cm^{-3}. The aerosol stream passed through a 23 cm-long, 1.25 cm ID PTFE tube wrapped in heating tape in order to volatilize the organics before entering the chemical ionization region of the mass spectrometer. The external temperature of the inlet was maintained at 135°C using a thermocouple and temperature controller (Staco Energy). No increase in signal was observed when the inlet temperature was increased to 160°C. Some experiments were performed with no inlet heating in order to test for species which were volatile at room temperature.

Flow through the aerosol inlet into the chemical ionization region was maintained at 3 SLPM using a critical orifice. The chemical ionization (CI) region consists of a 3.5 cm ID stainless steel manifold which is 3.8 cm long. Pressure in the CI region is maintained at 45–55 Torr by a mechanical pump (Varian DS302). For the negative ion detection scheme, I$^-$ reagent ions were generated by flowing dilute CH$_3$I (Alfa Aesar, 99.5%) in 3 SLPM N$_2$ (Tech Air, 99.999%) through a ^{210}Po ionizer (NRD). The ionizer was mounted perpendicular to the CI region. For detection with H$_3$O$^+\cdot$(H$_2$O)$_n$, ions were generated by flowing a combined stream of 2 SLPM N$_2$ bubbled through Millipore water and 3 SLPM dry N$_2$ through the ionizer. Ion-neutral reaction times were 20–30 ms. For the H$_3$O$^+\cdot$(H$_2$O)$_n$ detection scheme, the predominant peaks in our spectra are H$_3$O$^+\cdot$(H$_2$O)$_2$ at 55 amu and H$_3$O$^+\cdot$(H$_2$O)$_3$ at 73 amu. The reagent ions react with the neutral species through proton transfer (Hearn and Smith, 2004a):

$$H_3O^+\cdot(H_2O)_n + R \rightarrow RH^+ + (H_2O)_{n+1} \tag{1}$$

or ligand switching (Blake et al., 2009):

$$H_3O^+\cdot(H_2O)_n + R \rightarrow H_3O^+\cdot R + (H_2O)_n \tag{2}$$
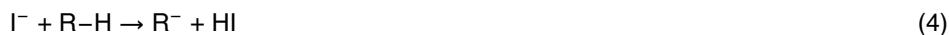
and the species are then detected as the protonated analyte molecule or its cluster with H$_2$O. In the I$^-$ detection scheme the analyte molecules form clusters with I$^-$ via a ligand-switching reaction:

$$I^-\cdot H_2O + R \rightarrow I^-\cdot R + H_2O \tag{3}$$

or they are ionized via proton abstraction:

$$I^- + R\text{–}H \rightarrow R^- + HI \tag{4}$$

Ions passed from the CI region through a 0.05 cm-ID charged orifice into a collisional dissociation chamber (CDC) which was maintained at 5 Torr by a mechanical pump (Varian DS402). Ions may be accelerated through this region using a series of biased cylindrical lenses in order to control clustering. The CDC is separated from the MS prechamber ($\sim 10^{-4}$ Torr) by a second charged orifice plate (ID=0.05 cm). The prechamber contains an ion optics assembly (Extrel CMS) and is separated by a 0.2 cm-ID orifice from the final chamber ($\sim 10^{-7}$ Torr) which houses the 19 mm quadrupole and detector (Extrel CMS). The final two chambers are differentially pumped by identical turbomolecular pumps (Varian TV-301 Navigator) backed by a single mechanical pump (Varian DS302). For regular operation the RF operating frequency for the mass spectrometer was 1.2 MHz; for high mass mode a 0.88 MHz RF supply was used (Extrel CMS).

The instrument was calibrated using aerosol-phase succinic acid (C$_4$H$_6$O$_4$). Aerosols were generated by atomizing a solution of 0.001 M succinic acid in Millipore water. Since the liquid water content of the aerosol particles was not known, we assume that the aerosol mass measured by the SMPS was comprised of 100% succinic acid and report the calculated sensitivity and detection limit values as lower and upper limits, respectively. The instrument sensitivity to aerosol-phase succinic acid was measured using the I$^-$ detection scheme to be ≥ 100 Hz ppt^{-1} with a detection limit of ≤ 0.01 µg m^{-3}. Using the H$_3$O$^+\cdot$(H$_2$O)$_n$ scheme, the sensitivity to succinic acid was ≥ 66 Hz ppt^{-1} and the detection limit was ≤ 0.02 µg m^{-3}.

2.2 DFT calculations

Geometry optimizations and energy calculations were performed using Jaguar 6.0 (Schrodinger, Inc.) with the ChemBio3D interface (CambridgeSoft) in order to evaluate

the interactions of proposed product molecules with I$^-$ for CIMS detection. Density functional theory was used with the B3LYP functional and the ERMLER2 basis set, which allows the treatment of iodine via the use of effective core potentials (Lajohn et al., 1987). The free energy change for the ligand-switching reaction (Eq. 3) or proton abstraction (Eq. 4) was calculated. For the ligand switching reaction several geometries for the cluster of the analyte molecule with I$^-$ were tested for each species, and in some cases several stable cluster geometries (local minima) were found. In each case, ΔG for the lowest-energy cluster geometry (global minimum) is reported. The free energy values reported here are from the output of the 298.15 K vibrational frequency calculation and no further corrections were applied.

3   Results and discussion

Representative Aerosol-CIMS mass spectra for the methylglyoxal/NaCl and methylglyoxal/(NH$_4$)$_2$SO$_4$ systems using I$^-$ or H$_3$O$^+\cdot$(H$_2$O)$_n$ as the reagent ion are shown in Figs. 3–6. The spectra represented in these figures have mass resolution of 1 amu except as noted; peak assignments were made using 0.5 amu resolution spectra.

3.1   Negative ion detection with I$^-$

A summary of proposed peak assignments for the mass spectra in Fig. 3 using I$^-$ as the reagent ion can be found in Table 1. Most of the peaks in the methylglyoxal/(NH$_4$)$_2$SO$_4$ mass spectrum are also found in the methylglyoxal/NaCl spectrum. Increased signal appears at 271.5, 273.5, and 289.5 amu in the methylglyoxal/(NH$_4$)$_2$SO$_4$ spectrum. Peaks unique to methylglyoxal/(NH$_4$)$_2$SO$_4$ include 225.2 and 275.6 amu. The peak at 217.3 amu is consistent with the cluster of I$^-$ with singly hydrated methylglyoxal. The presence of multiple peaks >217.3 amu is indicative of dimer formation.

3.1.1   DFT calculations

I$^-$ has previously been used as a reagent ion with Aerosol-CIMS to detect organic acids in aerosols (McNeill et al., 2007, 2008). Since the product species expected to be present in this reactive system (methylglyoxal, acetal/hemiacetal oligomers, aldol condensation oligomers) have not been previously detected via the I$^-$ ionization scheme, we performed ab initio calculations in order to characterize the interaction of proposed product species with I$^-$. The results are summarized in Table 2. Optimized geometries and calculated energies for each species can be found in the Supplementary Material (http://www.atmos-chem-phys-discuss.net/9/15567/2009/acpd-9-15567-2009-supplement.pdf). Our calculations show that the formation of clusters between I$^-$ and several of the acetal and hemiacetal species proposed by Zhao et al. (2006) via ligand switching with I$^-\cdot$H$_2$O is thermodynamically favorable, particularly when two or more hydroxyl moieties are available to interact with I$^-$ simultaneously. This is also the case for hydrated methylglyoxal species. Non-hydrated methylglyoxal is not predicted to form strong clusters with or be ionized by I$^-$, and therefore we do not expect to detect it using this approach. Aldol addition products from either pathway (e.g. species (d) or (h) from Table 2), if present, should be detected as their clusters with I$^-$. The only aldol condensation products which we predict to form strong clusters with I$^-$ are those species which terminate in a carboxylic acid group (e.g. species (f) from Table 2). We do not expect to observe products of aldol pathway 2 (Fig. 1) such as species (c) from Table 2 with this ionization scheme.

3.1.2   Volatile species

The peaks at 173.0, 190.1, and 217.3 amu were present in the same magnitude whether the volatilization inlet heat was turned on or off, indicating that these signals are associated with volatile species. The signal observed at 173.0 amu is consistent with formic acid (I$^-\cdot$HCOOH). Gas-phase formic acid has been previously observed to be an oxidation product of organic acids in aerosols; it was detected at this mass using Aerosol-CIMS with the same ionization scheme used here (McNeill et al., 2008). The

signal we observe at 190.1 amu is consistent with a molecular formula of $I^- \cdot CH_5O_2N$. The mechanism for formation of this product is unknown; it could be a fragment or decomposition product of a larger compound.

3.1.3 (Hemi)acetals and aldol condensation products

The peak at 271.5 amu is attributed to the molecular formula $I^- \cdot C_6H_8O_4$, which could correspond to the pathway 1 aldol condensation dimers or pathway 2 aldol addition products (Fig. 1 and Table 1). 289.5 amu is consistent with $I^- \cdot C_6H_{10}O_5$, and therefore can be matched to acetal and hemiacetal dimers proposed by others (Nemet et al., 2004; Loeffler et al., 2006; Zhao et al., 2006) or pathway 1 aldol addition products. Small amounts of signal at both of these masses are present in the methylglyoxal/NaCl spectrum, and temperature control experiments indicate that these species are semivolatile.

Since succinic acid, an organic diacid, is expected to cluster strongly with I^- we may assume that the instrument sensitivity to succinic acid ($100\,Hz\,ppt^{-1}$) is an upper limit for the sensitivity to these species. Using this assumption and the results of the kinetics study, we estimate lower bounds for the production rates of the species at 271.5 and 289.5 to be $\geq 10^{-3}\,M\,min^{-1}$ and $\geq 10^{-2}\,M\,min^{-1}$ in the particle, respectively. Using the model of dimerization presented in Schwier et al. (2009), and assuming that the aerosol is concentrated to 65 wt% $(NH_4)_2SO_4$ after equilibrating at 60% RH (Tang and Munkelwitz, 1994), we estimate the dimerization rate constants to be $\sim 10^{-4}\,M^{-1}\,min^{-1}$ and $\sim 10^{-3}\,M^{-1}\,min^{-1}$ for the species at 271.5 amu and 289.5 amu, respectively.

The peaks at 273.5 and 275.6 amu are assigned the molecular formulas $I^- \cdot C_6H_{10}O_4$ and $I^- \cdot C_6H_{12}O_4$, respectively. These molecular formulas, since they each contain six carbons, are consistent with the addition of two methylglyoxal monomers. Possible structures are shown in Table 1, but the formation mechanisms of these species in the methylglyoxal/$(NH_4)_2SO_4$ system are not known.

15575

3.1.4 Sulfur-containing species

The peak at 225.2 amu features a satellite peak at 227.2 amu with an abundance roughly consistent with the expected 95:4 ratio of the stable isotopes of sulfur ^{32}S and ^{34}S (Fig. 4), suggesting a compound containing sulfur. Either a molecule with a molecular weight of 226.2 amu (in the case of proton abstraction) or 98.3 amu (in the case of a cluster with I^-) would be consistent with the 225.2 amu mass-to-charge ratio. The species with m/z 225.2 was observed to be nonvolatile at room temperature. One possible molecular formula for this species is $C_6H_9O_7S^-$. The proposed structure for the $C_6H_9O_7S^-$ organosulfate species is shown in Table 1. Our DFT calculations predict that proton abstraction from the sulfate group by I^-, rather than clustering via the ligand-switching reaction, is thermodynamically favorable for this species. Kinetics studies show that the signal at 225.2 amu develops within approximately 30 min of mixing. Assuming an upper limit sensitivity of $100\,Hz\,ppt^{-1}$ for this species we can estimate a production rate of $\geq 4 \times 10^{-3}\,M\,min^{-1}$ in the particle.

H_2SO_4 may cluster with I^- or undergo proton abstraction. $I^- \cdot H_2SO_4$, if present, would also appear at 225.2 amu and display a satellite peak at 227.2 amu. In order to test for this possibility a control experiment was performed in which a 0.2 M $(NH_4)_2SO_4$ solution at pH=2 (similar to the conditions of the solutions with methylglyoxal) was atomized and analyzed using Aerosol-CIMS. There was no peak at 225.2 amu in the spectrum of the control, suggesting that the observed peak in the methylglyoxal/$(NH)_2SO_4$ spectrum cannot be attributed to inorganic sulfate or sulfuric acid. Hearn and Smith (2006b) previously used Aerosol-CIMS with SF_6^- as the parent ion and a volatilization temperature of 220°C to detect aerosol sulfate (as HSO_4^-, 97 amu). We observed a small (~ 300 cps) peak at 97 amu in the methylglyoxal/$(NH_4)_2SO_4$ spectra but not in the control experiment. We note that organosulfates have previously been observed to decompose during negative ion mass spectrometry to generate HSO_4^- (Attygalle et al., 2001).

15576

3.2 Positive ion detection using $H_3O^+ \cdot (H_2O)_n$

$H_3O^+ \cdot (H_2O)_n$ is commonly used to detect VOCs, including methylglyoxal (Zhao et al., 2006; Blake et al., 2009) and has been used to detect volatilized aerosol organics including levoglucosan from tobacco and wood smoke, limonene SOA (Hearn and Smith, 2004a) and pyridine (Thornberry et al., 2009). Table 3 lists the proposed peak assignments for the spectra in Fig. 5 which were obtained using $H_3O^+(H_2O)_n$ as the reagent ion. More peaks appear in these spectra than in those obtained using I^- as a reagent ion because proton transfer via $H_3O^+(H_2O)_n$ is favorable for a wider variety of organics than ligand switching or proton abstraction via I^- is. Most of the peaks observed are common to the methylglyoxal/$(NH_4)_2SO_4$ and methylglyoxal/NaCl mass spectra. Signal at 94.9, 98.8, 125.9, 143.8, and 163.0 is significantly higher in the methylglyoxal/$(NH_4)_2SO_4$ spectrum. Other notable peaks include 165.0, 167.1, 181.2, and 235.3 amu. The peaks at $m/z \leq 167.1$ amu (except for 98.8 amu) were present in the mass spectrum when the volatilization inlet heat was turned off, indicating that these signals are associated with volatile or semivolatile species.

Methylglyoxal has been detected previously using proton transfer mass spectrometry (Zhao et al., 2006). In our experiment, the expected m/z for methylglyoxal coincided with that of one of the parent ions, $H_3O^+ \cdot (H_2O)_3$, at 73.1 amu. Water clusters of methylglyoxal or the hydrated forms would correspond with $H_3O^+ \cdot (H_2O)_4$ and $H_3O^+ \cdot (H_2O)_5$ at 91.1 and 109.1 amu, respectively. A small signal is observed at 109.1 amu.

The peak at 94.9 amu is consistent with a molecular formula of $C_2H_7O_4^+$. This is likely a decomposition product or fragment of a larger compound.

3.2.1 (Hemi)acetals and aldol condensation products

The peak at 125.9 amu is consistent with the molecular formula $C_6H_8O_2N^+$, corresponding to a type 2 aldol condensation product with a single imine substitution. The peak at 143.8 is consistent with a water cluster or aldol addition precursor of that species, or else a type 1 aldol condensation product with one amine or imine substitution. The peak at 163.0 amu corresponds to $C_6H_{11}O_5^+$; the species which appear

at 289.5 amu in the I^- spectrum should appear at this mass. Alternatively, it could be the water cluster of $C_6H_9O_4^+$, the type 1 aldol condensation or type 2 aldol addition products which were observed at 271.5 amu in the I^- spectrum. Acetal and hemiacetal species also appear at 181.2 and 235.3 amu (see Table 3).

The peaks at 165.0 and 167.1 amu correspond to $C_6H_{13}O_5^+$ and $C_6H_{15}O_5^+$, respectively, or the water clusters of $C_6H_{11}O_4^+$ and $C_6H_{13}O_4^+$. These molecular formulas are consistent with methylglyoxal dimers but the structure and formation mechanism are not known for these species.

3.2.2 Sulfur-containing products

No peak at 227 amu, which would correspond to $C_6H_{11}O_7S^+$, was observed in the methylglyoxal/$(NH_4)_2SO_4$ spectrum as detected using $H_3O^+(H_2O)_n$. To our knowledge organosulfates have not been previously detected using proton transfer ionization.

A peak was observed at 98.8 amu, but no satellite peak was present at 100.8 amu. The signal did not appear in the methylglyoxal/NaCl spectrum. Control experiments confirmed that no peak appeared at 98.8 amu when acidified $(NH_4)_2SO_4$ without methylglyoxal was present in the atomizer solution. Proton transfer ionization is not expected to allow detection of inorganic sulfate or sulfuric acid at this mass. Molecular formulas consistent with this mass-to-charge ratio include $C_6H_{11}O^+$, $C_5H_7O_2^+$, or $C_4H_3O_3^+$.

3.2.3 High-molecular-weight species

In order to test our ability to detect high-molecular-weight organics with the Aerosol-CIMS technique, we analyzed aerosols containing NaCl and PEG (570–630 amu) in high-mass mode. We observed two sets of peaks separated by 44($\pm$1) amu (one ethylene oxide unit): {475.8, 518.9, 563.7, 607.4, and 651.5} and {502.4, 546.6, 590.9, 635.1}. This is consistent with the observations of Bogan et al. (2007).

For methylglyoxal/$(NH_4)_2SO_4$ we observed peaks from 536.6–759.5 amu in high-mass mode using $H_3O^+(H_2O)_n$ as the reagent ion (see Fig. 6). The peaks were sep-

arated by 74 amu, which could correspond to a unit of $C_3H_6O_2$. We did not observe non-background signal for $m/z>300$ amu when using I^- as the reagent ion. We previously observed that glyoxal forms oligomers of 500–600 amu in aqueous solution when ammonium sulfate is present (Shapiro et al., 2009). Kalberer et al. (2004) observed oligomers up to ~750 amu for aqueous methylglyoxal using LDI-MS.

4 Conclusions and atmospheric implications

The results of this study confirm that ammonium sulfate plays an active role in the chemistry of methylglyoxal in aqueous aerosol mimics. Our observations of nitrogen-substituted organics show that ammonium is a reactant in this system, and not just a catalyst. This previously unidentified formation pathway adds to the recent reports of heterogeneous SOA formation pathways (Nozière et al., 2009; Shapiro et al., 2009; Galloway et al., 2009; De Haan et al., 2009a,b) that could contribute to the nitrogen-containing aerosol organics which have been observed in field studies (Denkenberger et al., 2007; Aiken et al., 2008).

Our observation of aldol condensation products confirms the predictions of Barsanti and Pankow (2004) and Krizner et al. (2009), and is consistent with our observation of light-absorbing products when NH_4^+ is present in this system (Schwier et al., 2009). Because of the dilution step in the aerosol sample preparation we infer that the formation of the acetal oligomer and aldol condensation species detected here is effectively irreversible.

We also have made a tentative identification of an organosulfate product. To our knowledge, organosulfate formation by methylglyoxal in ammonium sulfate aerosols has not been observed previously, although Liggio et al. (2005a,b) and Galloway et al. (2009) identified organosulfate products in ammonium sulfate aerosols exposed to gas phase glyoxal. Organosulfates have been identified in ambient aerosol (Gao et al., 2006; Iinuma et al., 2007; Surratt et al., 2007, 2008; Gomez-Gonzalez et al., 2008; Russell et al., 2009; Lukács et al., 2009). Lukács et al. (2009) observed that organosulfate mass concentrations were at a maximum for submicron aerosol size

15579

fractions, suggesting a link between organosulfate formation and heterogeneous SOA formation pathways.

Finally, we have demonstrated here that Aerosol-CIMS using I^- and $H_3O^+(H_2O)_n$ as the parent ions is suitable for the detection of the products of heterogeneous SOA formation by α-dicarbonyls, and high molecular weight organics up to 759 amu. This technique can be extended to aerosol chamber studies and, when coupled with a suitable aerosol collection or concentration technique, field studies.

References

Aiken, A. C., DeCarlo, P. F., Kroll, J. H., Worsnop, D. R., Huffman, J. A., Docherty, K. S., Ulbrich, I. M., Mohr, C., Kimmel, J. R., Sueper, D., Sun, Y., Zhang, Q., Trimborn, A., Northway, M., Ziemann, P. J., Canagaratna, M. R., Onasch, T. B., Alfarra, M. R., Prevot, A. S. H., Dommen, J., Duplissy, J., Metzger, A., Baltensperger, U., and Jimenez, J. L.: O/C and OM/OC ratios of primary, secondary, and ambient organic aerosols with high-resolution time-of-flight aerosol mass spectrometry, Environ. Sci. Technol., 42, 4478–4485, 2008.

Anttila, T., Kiendler-Scharr, A., Tillman, R., and Mentel, T. F.: On the reactive uptake of gaseous compounds by organic-coated aqueous aerosols: theoretical analysis and application to the heterogeneous hydrolysis of N_2O_5, J. Phys. Chem. A, 110, 10 435–10 443, 2006.

Attygalle, A. B., Garcia-Rubio, S., Ta, J., and Meinwald, J.: Collisionally-induced dissociation mass spectra of organic sulfate anions, J. Chem. Soc., Perkin Trans., 2, 498–506, 2001.

Barsanti, K. C. and Pankow, J. F.: Thermodynamics of the formation of atmospheric organic particulate matter by accretion reactions – 2. Dialdehydes, methylglyoxal, and diketones, Atmos. Environ., 39, 6597–6607, 2005.

Blake, R. S., Monks, P. S., and Ellis, A. M.: Proton-transfer reaction mass spectrometry, Chem. Rev., 109, 861–896, 2009.

Bogan, M. J., Patton, E., Srivastava, A., Martin, S., Fergenson, D. P., Steele, P. T., Tobias, H. J., Gard, E. E., and Frank, M.: Online aerosol mass spectrometry of single micrometer-sized particles containing poly(ethylene glycol), Rapid Commun. Mass Sp., 21, 1214–1220, 2007.

15580

Casale, M. T., Richman, A. R., Elrod, M. J., Garland, R. M., Beaver, M. R., and Tolbert, M. A.: Kinetics of acid-catalyzed aldol condensation reactions of aliphatic aldehydes, Atmos. Environ., 41, 6212–6224, 2007.

Cruz, C. N. and Pandis, S. N.: A study of the ability of pure secondary organic aerosol to act as cloud condensation nuclei, Atmos. Environ., 31, 2205–2214, 1997.

De Haan, D. O., Corrigan, A. L., Smith, K. W., Stroik, D. R., Turley, J. J., Lee, F. E., Tolbert, M. A., Jimenez, J. L., Cordova, K. E., and Ferrell, G. R.: Secondary organic aerosol-forming reactions of glyoxal with amino acids, Environ. Sci. Technol., 43, 2818–2824, 2009a.

De Haan, D. O., Tolbert, M. A., and Jimenez, J. L.: Atmospheric condensed-phase reactions of glyoxal with methylamine, Geophys. Res. Lett., 36, L11819, doi:10.1029/2009GL037441, 2009b.

Denkenberger, K. A., Moffet, R. C., Holecek, J. C., Rebotier, T. P., and Prather, K. A.: Real-time, single-particle measurements of oligomers in aged ambient aerosol particles, Environ. Sci. Technol., 41, 5439–5446, 2007.

Duplissy, J., Gysel, M., Alfarra, M. R., Dommen, J., Metzger, A., Prevot, A. S. H., Weingartner, E., Laaksonen, A., Raatikainen, T., Good, N., Turner, S. F., McFiggans, G., and Baltensperger, U.: Cloud forming potential of secondary organic aerosol under near atmospheric conditions, Geophys. Res. Lett., 35, L03818, doi:10.1029/2007GL031075, 2008.

Folkers, M., Mentel, T. F., and Wahner, A.: Influence of an organic coating on the reactivity of aqueous aerosols probed by the heterogeneous hydrolysis of N_2O_5, Geophys. Res. Lett., 30, 1644–1647, 2003.

Fu, T. M., Jacob, D. J., and Heald, C. L.: Aqueous-phase reactive uptake of dicarbonyls as a source of organic aerosol over eastern North America, Atmos. Environ., 43, 1814–1822, 2009.

Galloway, M. M., Chhabra, P. S., Chan, A. W. H., Surratt, J. D., Flagan, R. C., Seinfeld, J. H., and Keutsch, F. N.: Glyoxal uptake on ammonium sulphate seed aerosol: reaction products and reversibility of uptake under dark and irradiated conditions, Atmos. Chem. Phys., 9, 3331–3345, 2009, http://www.atmos-chem-phys.net/9/3331/2009/.

Gao, S., Surratt, J. D., Knipping, E. M., Edgerton, E. S., Shahgholi, M., and Seinfeld, J. H.: Characterization of polar organic components in fine aerosols in the southeastern United States: identity, origin, and evolution, J. Geophys. Res.-Atmos., 111(D14), D14314, doi:10.1029/2005JD006601, 2006.

Gomez-Gonzalez, Y., Surratt, J. D., Cuyckens, F., Szmigielski, R., Vermeylen, R., Jaoui, M.,

15581

Lewandowski, M., Offenberg, J. H., Kleindienst, T. E., Edney, E. O., Blockhuys, F., Van Alsenoy, C., Maenhaut, W., and Claeys, M.: Characterization of organosulfates from the photooxidation of isoprene and unsaturated fatty acids in ambient aerosol using liquid chromatography/(-)electrospray ionization mass spectrometry, J. Mass Spectrom., 43, 371–382, 2008.

Grosjean, D., Williams, E. L., and Grosjean, E.: Atmospheric chemistry of isoprene and of its carbonyl products, Environ. Sci. Technol., 27, 830–840, 1993.

Hartz, K. E. H., Rosenorn, T., Ferchak, S. R., Raymond, T. M., Bilde, M., Donahue, N. M., and Pandis, S. N.: Cloud condensation nuclei activation of monoterpene and sesquiterpene secondary organic aerosol, J. Geophys. Res.-Atmos., 110(D14), D14208, 2005.

Hearn, J. D., Lovett, A. J., and Smith, G. D.: Ozonolysis of oleic acid particles: evidence for a surface reaction and secondary reactions involving Criegee intermediates, Phys. Chem. Chem. Phys., 7, 501–511, 2005.

Hearn, J. D., Renbaum, L. H., Wang, X., and Smith, G. D.: Kinetics and Products from a reaction of Cl radicals with dioctyl sebacate (DOS) particles in O_2: a model for radical-initiated oxidation of organic aerosols, Phys. Chem. Chem. Phys., 9, 1–11, 2007.

Hearn, J. D. and Smith, G. D.: A chemical ionization mass spectrometry method for the online analysis of organic aerosols, Anal. Chem., 76, 2820–2826, 2004a.

Hearn, J. D. and Smith, G. D.: Kinetics and product studies for ozonolysis reactions of organic particles using aerosol CIMS, J. Phys. Chem. A, 108, 10019–10029, 2004b.

Hearn, J. D. and Smith, G. D.: Measuring rates of reaction in supercooled organic particles with implications for atmospheric aerosol, Phys. Chem. Chem. Phys., 7, 2549–2551, 2005.

Hearn, J. D. and Smith, G. D.: A mixed-phase relative rates technique for measuring aerosol reaction kinetics, Geophys. Res. Lett., 33, L17805, doi:10.1029/2006GL026963, 2006a.

Hearn, J. D. and Smith, G. D.: Reactions and mass spectra of complex particles using Aerosol CIMS, Int. J. Mass Spectrom., 258, 95–103, 2006b.

Hearn, J. D. and Smith, G. D.: Ozonolysis of mixed oleic acid/n-docosane particles: the roles of phase, morphology, and metastable states, J. Phys. Chem. A, 111, 11 059–11 065, 2007.

Iinuma, Y., Muller, C., Berndt, T., Boge, O., Claeys, M., and Herrmann, H.: Evidence for the existence of organosulfates from beta-pinene ozonolysis in ambient secondary organic aerosol, Environ. Sci. Technol. 41, 6678–6683, 2007.

Jang, M. S., Czoschke, N. M., Lee, S., and Kamens, R. M.: Heterogeneous atmospheric aerosol production by acid-catalyzed particle-phase reactions, Science, 298, 814–817, 2002.

15582

Kalberer, M., Paulsen, D., Sax, M., Steinbacher, M., Dommen, J., Prevot, A. S. H., Fisseha, R., Weingartner, E., Frankevich, V., Zenobi, R., and Baltensperger, U.: Identification of polymers as major components of atmospheric organic aerosols, Science, 303, 1659–1662, 2004.

King, S. M., Rosenoern, T., Shilling, J. E., Chen, Q., and Martin, S. T.: Cloud condensation nucleus activity of secondary organic aerosol particles mixed with sulfate, Geophys. Res. Lett., 34, L24806, doi:10.1029/2007GL030390, 2007.

Krizner, H. E., De Haan, D. O., and Kua, J.: Thermodynamics and kinetics of methylglyoxal dimer formation: a computational study, J. Phys. Chem. A, 113, 6994–7001, 2009.

Kroll, J. H., Ng, N. L., Murphy, S. M., Varutbangkul, V., Flagan, R. C., and Seinfeld, J. H.: Chamber studies of secondary organic aerosol growth by reactive uptake of simple carbonyl compounds, J. Geophys. Res.-Atmos., 110(D23), D23207, doi:10.1029/2005JD006004, 2005.

Lajohn, L. A., Christiansen, P. A., Ross, R. B., Atashroo, T., and Ermler, W. C.: Abinitio relativistic effective potentials with spin orbit operators .3. Rb Through Xe, J. Chem. Phys., 87, 2812–2824, 1987.

Liggio, J., Li, S. M., and McLaren, R.: Heterogeneous reactions of glyoxal on particulate matter: identification of acetals and sulfate esters, Environ. Sci. Technol., 39, 1532–1541, 2005a.

Liggio, J., Li, S. M., and McLaren, R.: Reactive uptake of glyoxal by particulate matter, J. Geophys. Res.-Atmos., 110(D10), D10304, doi:10.1029/2004JD005113, 2005b.

Loeffler, K. W., Koehler, C. A., Paul, N. M., and De Haan, D. O.: Oligomer formation in evaporating aqueous glyoxal and methyl glyoxal solutions, Environ. Sci. Technol., 40, 6318–6323, 2006.

Lukács, H., Gelencsér, A., Hoffer, A., Kiss, G., Horváth, K., and Hartyáni, Z.: Quantitative assessment of organosulfates in size-segregated rural fine aerosol, Atmos. Chem. Phys., 9, 231–238, 2009, http://www.atmos-chem-phys.net/9/231/2009/.

McNeill, V. F., Wolfe, G. M., and Thornton, J. A.: The oxidation of oleate in submicron aqueous salt aerosols: evidence of a surface process, J. Phys. Chem. A, 111, 1073–1083, 2007.

McNeill, V. F., Yatavelli, R. L. N., Stipe, C. B., and Landgrebe, O.: Heterogeneous OH oxidation of palmitic acid in single component and internally mixed aerosol particles: vaporization and the role of particle phase, Atmos. Chem. Phys., 8, 5465–5476, 2008, http://www.atmos-chem-phys.net/8/5465/2008/.

Michaud, V., El Haddad, I., Liu, Y., Sellegri, K., Laj, P., Villani, P., Picard, D., Marchand, N., and Monod, A.: In-cloud processes of methacrolein under simulated conditions – Part 3: Hygroscopic and volatility properties of the formed Secondary Organic Aerosol, Atmos. Chem.

15583

Phys. Discuss., 9, 6451–6482, 2009, http://www.atmos-chem-phys-discuss.net/9/6451/2009/.

Nemet, I., Vikic-Topic, D., and Varga-Defterdarovic, L.: Spectroscopic studies of methylglyoxal in water and dimethylsulfoxide, Bioorg. Chem., 32, 560–570, 2004.

Nozière, B., Dziedzic, P., and Cordova, A.: Formation of secondary light-absorbing "fulvic-like" oligomers: a common process in aqueous and ionic atmospheric particles?, Geophys. Res. Lett., 34, L21812, doi:10.1029/2007GL031300, 2007.

Nozière, B., Dziedzic, P., and Cordova, A.: Products and kinetics of the liquid-phase reaction of glyoxal catalyzed by ammonium ions (NH_4^+), J. Phys. Chem. A, 113, 231–237, 2009.

Nozière, B. and Esteve, W.: Light-absorbing aldol condensation products in acidic aerosols: Spectra, kinetics, and contribution to the absorption index, Atmos. Environ., 41, 1150–1163, 2007.

Paulsen, D., Dommen, J., Kalberer, M., Prevot, A. S. H., Richter, R., Sax, M., Steinbacher, M., Weingartner, E., and Baltensperger, U.: Secondary organic aerosol formation by irradiation of 1,3,5-trimethylbenzene-NO_x-H_2O in a new reaction chamber for atmospheric chemistry and physics, Environ. Sci. Technol., 39, 2668–2678, 2005.

Russell, L. M., Takahama, S., Liu, S., Hawkins, L. N., Covert, D. S., Quinn, P. K., and Bates, T. S.: Oxygenated fraction and mass of organic aerosol from direct emission and atmospheric processing measured on the R/V Ronald Brown during TEXAQS/GoMACCS 2006, J. Geophys. Res.-Atmos., 114, D00F05, doi:10.1029/2008JD011275, 2009.

Saathoff, H., Naumann, K. H., Schnaiter, M., Schock, W., Mohler, O., Schurath, U., Weingartner, E., Gysel, M., and Baltensperger, U.: Coating of soot and $(NH_4)_2SO_4$ particles by ozonolysis products of alpha-pinene, J. Aerosol Sci., 34, 1297–1321, 2003.

Schwier, A. N., Shapiro, E. L., Sareen, N., and McNeill, V. F.: Secondary organic material formed by methylglyoxal in aqueous aerosol mimics – Part 1: Surface tension depression and light-absorbing products, Atmos. Chem. Phys. Discuss., 9, 15541–15565, 2009, http://www.atmos-chem-phys-discuss.net/9/15541/2009/.

Shapiro, E. L., Szprengiel, J., Sareen, N., Jen, C. N., Giordano, M. R., and McNeill, V. F.: Light-absorbing secondary organic material formed by glyoxal in aqueous aerosol mimics, Atmos. Chem. Phys., 9, 2289–2300, 2009, http://www.atmos-chem-phys.net/9/2289/2009/.

Smith, D. F., Kleindienst, T. E., and McIver, C. D.: Primary product distributions from the reaction of OH with *m*-, *p*-xylene, 1,2,4- and 1,3,5-trimethylbenzene, J. Atmos. Chem., 34, 339–364, 1999.

15584

Surratt, J. D., Gomez-Gonzalez, Y., Chan, A. W. H., Vermeylen, R., Shahgholi, M., Kleindi-enst, T. E., Edney, E. O., Offenberg, J. H., Lewandowski, M., Jaoui, M., Maenhaut, W., Claeys, M., Flagan, R. C., and Seinfeld, J. H.: Organosulfate formation in biogenic secondary organic aerosol, J. Phys. Chem. A, 112, 8345–8378, 2008.

Tang, I. N. and Munkelwitz, H. R.: Water activities, densities, and refractive-indexes of aqueous sulfates and sodium-nitrate droplets of atmospheric importance, J. Geophys. Res.-Atmos., 99(D9), 18801–18808, 1994.

Tuazon, E. C., Macleod, H., Atkinson, R., and Carter, W. P. L.: Alpha-dicarbonyl yields from the NO$_x$-air photooxidations of a series of aromatic-hydrocarbons in air, Environ. Sci. Technol., 20, 383–387, 1986.

Thornberry, T., Murphy, D. M., Thomson, D. S., de Gouw, J. A., Warneke, C., Bates, T. S., Quinn, P. K., and Coffman, D.: Measurement of aerosol organic compounds using a novel collection/thermal-desorption PTR-ITMS instrument, Aerosol Sci. Technol., 43, 486–501, 2009.

Tuazon, E. C., Macleod, H., Atkinson, R., and Carter, W. P. L.: Alpha-dicarbonyl yields from the NO$_x$-air photooxidations of a series of aromatic-hydrocarbons in air, Environ. Sci. Technol., 20, 383–387, 1986.

Volkamer, R., Jimenez, J. L., San Martini, F., Dzepina, K., Zhang, Q., Salcedo, D., Molina, L. T., Worsnop, D. R., and Molina, M. J.: Secondary organic aerosol formation from anthro-pogenic air pollution: rapid and higher than expected, Geophys. Res. Lett., 33, L17811, doi:10.1029/2006GL026899, 2006.

Volkamer, R., San Martini, F., Molina, L. T., Salcedo, D., Jimenez, J. L., and Molina, M. J.: A missing sink for gas-phase glyoxal in Mexico City: formation of secondary organic aerosol, Geophys. Res. Lett., 34, L19807, doi:10.1029/2007GL030752, 2007.

Volkamer, R., Ziemann, P. J., and Molina, M. J.: Secondary Organic Aerosol Formation from Acetylene (C$_2$H$_2$): seed effect on SOA yields due to organic photochemistry in the aerosol aqueous phase, Atmos. Chem. Phys., 9, 1907–1928, 2009, http://www.atmos-chem-phys.net/9/1907/2009/.

Zhao, J., Levitt, N. P., Zhang, R. Y., and Chen, J. M.: Heterogeneous reactions of methylglyoxal in acidic media: Implications for secondary organic aerosol formation, Environ. Sci. Technol., 40, 7682–7687, 2006.
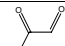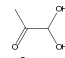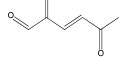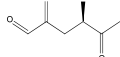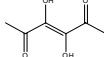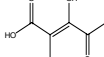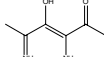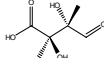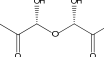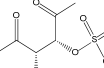
15585

Table 1. Proposed peak assignments for Aerosol-CIMS mass spectra with I$^-$ as the reagent ion. See text for details.

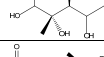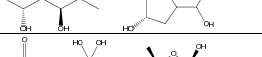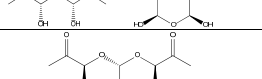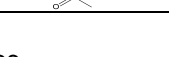| Peak (amu) ± 0.5 amu	Molecular formula	Possible Structure(s)
217.3	I$^-$C$_3$H$_6$O$_3$	
225.2	C$_6$H$_9$O$_7$S$^-$	
271.5	I$^-$C$_6$H$_8$O$_4$	
273.5	I$^-$C$_6$H$_{10}$O$_4$	
275.6	I$^-$C$_6$H$_{12}$O$_4$	
289.5	I$^-$C$_6$H$_{10}$O$_5$	
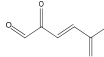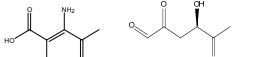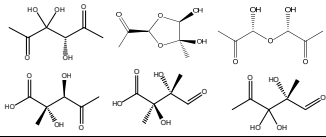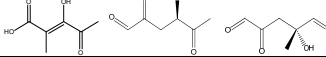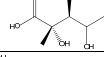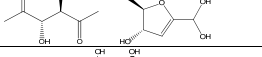
15586

Table 2. Proposed reaction products. Predictions for the free energy change of the ligand switching reaction with $I^- \cdot H_2O$ to form a cluster with I^- based on DFT B3LYP/ERMLER2 calculations are shown. Strong clustering is indicated in bold.

	Molecule	Molecular formula	Molecular weight (amu)	DFT ΔG (kJ mol^{-1}) $R + I^- \cdot H_2O \rightarrow I^- R + H_2O$
a)		$C_3H_4O_2$	72.1	-3.14
b)		$C_3H_6O_3$	90.1	**-44.1**
c)		$C_6H_6O_3$	126.1	-16.1
d)		$C_6H_8O_4$	144.1	**-34.3**
e)		$C_6H_8O_4$	144.1	-1.07
f)		$C_6H_8O_4$	144.1	**-49.2**
g)		$C_6H_{10}O_2N_2$	141.2	-7.77
h)		$C_6H_{10}O_5$	162.1	**-65.2**
i)		$C_6H_{10}O_5$	162.1	**-65.7**
j)		$C_6H_{10}O_7S$	226.2	H-abstraction from the sulfate group:**-118.0**

15587

Table 3. Proposed peak assignments for Aerosol-CIMS mass spectra with $H_3O^+ \cdot (H_2O)_n$ as the reagent ion. See text for details.

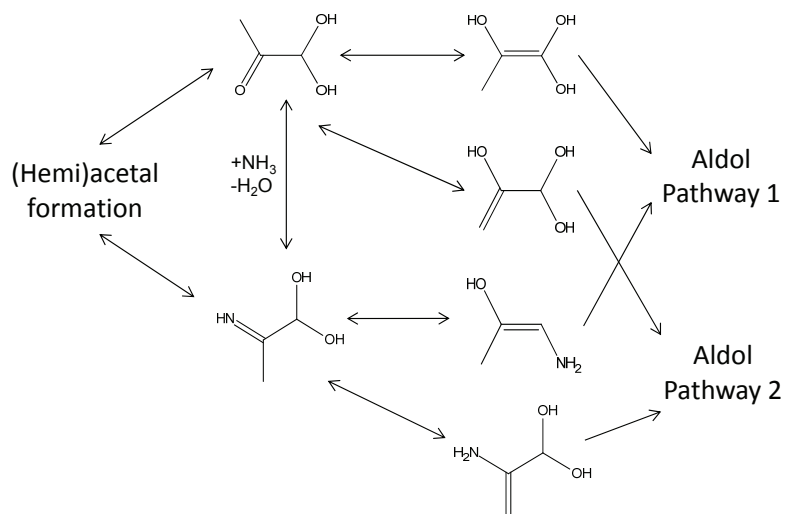| Peak (amu) ± 0.5 amu	Molecular formula	Possible Structure(s)
125.9	$C_6H_8O_2N^+$	
143.8	$C_6H_{10}O_3N^+$ $C_6H_8O_2N^+ \cdot H_2O$	
163.0	$C_6H_{11}O_5^+$	
	$C_6H_9O_4^+ \cdot H_2O$	
165.0	$C_6H_{13}O_5^+$	
	$C_6H_{11}O_4^+ \cdot H_2O$	
167.1	$C_6H_{15}O_5^+$	
	$C_6H_{13}O_4^+ \cdot H_2O$	
181.2	$C_6H_{13}O_6^+$ $C_6H_{11}O_5^+ \cdot H_2O$	
235.3	$C_9H_{15}O_7^+$	

15588
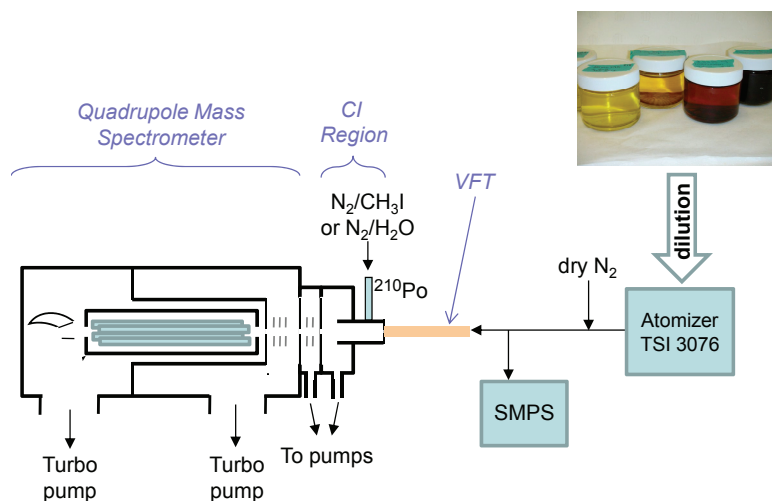
Fig. 1. Reaction pathways for methylglyoxal.

15589

Fig. 2. Schematic of Aerosol-CIMS setup for the detection of products formed during the reactions of methylgyoxal in aqueous solution with $(NH_4)_2SO_4$ or NaCl. SMPS: scanning mobility particle sizer, VFT: volatilization flow tube, CI: chemical ionization. See text for details.
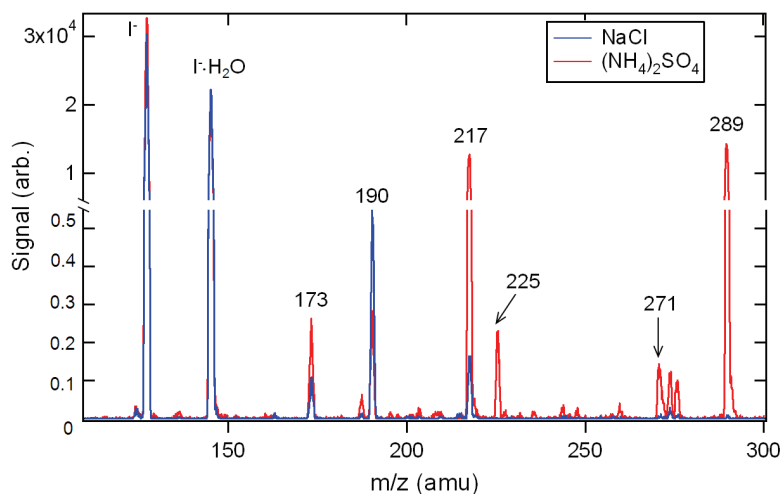
Fig. 3. Negative-ion mass spectrum of aerosolized aqueous solutions initially containing methylglyoxal and NaCl (blue) or $(NH_4)_2SO_4$ (red) (see text for details). Select product species were detected using I^- as the reagent ion. Peaks associated with I^- and its cluster with H_2O as well as the mass-to-charge ratios of product peaks are labeled.
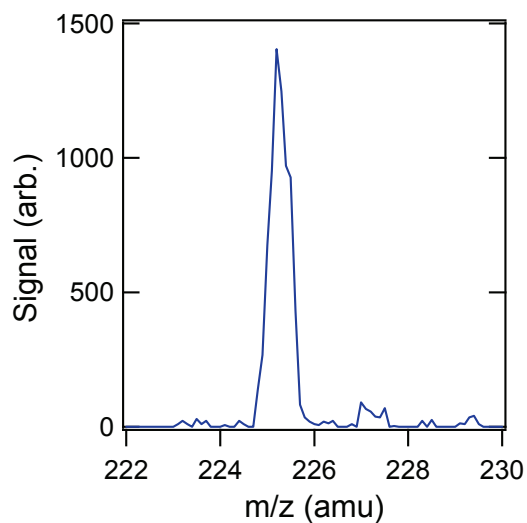
15591

Fig. 4. Detail of a 0.5 amu-resolution negative ion mass spectrum of aerosolized methyl-glyoxal/$(NH_4)_2SO_4$ solution. A peak at 225.2 amu and a satellite peak at 227.2 amu are shown.
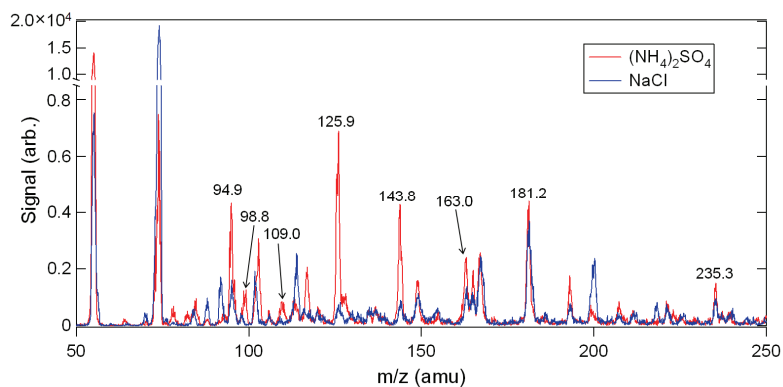
Fig. 5. Positive ion mass spectrum of aerosolized aqueous solutions initially containing methyl-glyoxal and NaCl (blue) or $(NH_4)_2SO_4$ (red). $H_3O^+ \cdot (H_2O)_n$ was the chemical ionization reagent. The mass-to-charge ratios of select product peaks are labeled.
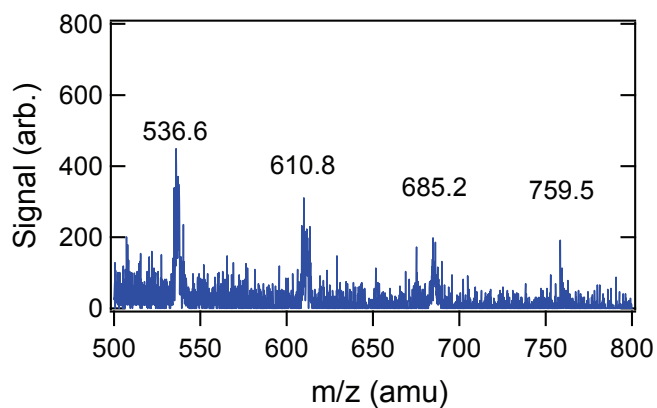
15593

Fig. 6. Detail of a positive ion mass spectrum of an aerosolized methylglyoxal/$(NH_4)_2SO_4$ solution. Spectrum was taken in high-mass mode with $H_3O^+ \cdot (H_2O)_n$ as the reagent ion.